Chinese Chemical Letters 36 (2025) 110353

Contents lists available at ScienceDirect

Chinese Chemical Letters

journal homepage: www.elsevier.com/locate/cclet

Surface controllable wettability using amphiphilic rotaxane molecular shuttles

Dongpu Wu, Zheng Yang, Yuchen Xia, Lulu Wu, Yingxia Zhou, Caoyuan Niu, Puhui Xie, Xin Zheng, Zhanqi Cao*

College of Science, Henan Agricultural University, Zhengzhou 450002, China

ARTICLE INFO

Article history:
Received 7 May 2024
Revised 5 August 2024
Accepted 21 August 2024
Available online 23 August 2024

Keywords:
Amphiphilic [2]rotaxane
Controllable wettability
Stimuli-responsive

ABSTRACT

Herein, an alkyne-terminated acid/base responsive amphiphilic [2]rotaxane shuttle was synthesized, and then modified onto the glass surface through "click" reaction. The XPS N 1s spectrum and contact-angle measurement were performed to prove the successful immobilization. The amphiphilic [2]rotaxane functionalized surface presented controllable wettability responding to external acid-base stimuli. This bistable rotaxane modified material system promoted the practical application of molecular machines.

With the rapid development of supramolecular chemistry, intelligent responsive organic functional materials constructed based on host-guest recognition interaction have become a hot spot research area in material chemistry [1,2]. As the typical class of organic functional materials, rotaxane molecular shuttles consist of a rod-like component and a ring-like component combined by host-guest recognition, and the two ends are blocked by large blocking groups. Under certain external stimuli, the ring component can make reversible shuttle motion along the rod-like component. Due to the good stimulus responsiveness of rotaxane molecular shuttles, it has important applications in the field of building intelligent responsive functional materials [3]. Artificial molecular machines (AMMs) have gained immense development during the past decades [4-6]. And AMMs materials are endowed with increasingly exquisite structures and intelligent functions [7-9]. Whereas, the perspective trend is to demonstrate that microcosmic molecular motion can be integrated and amplified into useful work [10,11]. Accordingly, AMMs are widely used in various domains, for instance, they are applied to transmembrane transport [12-14], polymer materials [15-18], molecular valves [19,20], noble metal recovery [21,22], mitochondrial imaging [23,24]. As the expanded applications of AMMs, the research has evolved from traditional solution systems to surface, interface and solid-phase [25,26]. Last few years, the use of AMMs systems for surface self-assembly has become a focus of research topics in the field of supramolecular chemistry [27]. Self-assembled monolayer (SAM) is a promising strategy, which enables the application to self-cleaning surfaces [28,29], lab-on-chip systems [30,31], microfluidic tools [32], optical lenses [33], and so on [34].

Bistable [2]rotaxane [35-37], as one type of traditional AMMs, in which the host macrocycle component could thread between two independent recognition sites under external stimuli and show controllable functions. In our previous work [38], the bistable [2]rotaxane was used as the backbone to construct amphiphilic [2]rotaxane and self-assembled into different spherical vesicles and worm-like micelles morphologies using acid/base stimuli in solution. And here, the analogous amphiphilic [2]rotaxane was further modified onto the surface to control the wettability responding to external stimuli. The acid-base stimulation could control the distance between hydrophilic and hydrophobic groups and then affect surface wettability. This work further promotes the development of AMMs towards surface interfaces.

Herein, we designed and synthesized an alkyne-terminated amphiphilic bistable [2]rotaxane molecular shuttle (**R-3**), in which the other end functionalized with hydrophobic alkyl chain and the macrocycle component modified with hydrophilic tetraethylene glycol monomethyl ether, and then it was attached to glass surface preparing self-assembled monolayers (**SAM-R-3**) through the well-known copper(I)-catalyzed Huisgen 1,3-dipolar cycloaddition reaction (Scheme 1) [39]. There are two typical recognition sites, namely dibenzylammonium (DBA) and *N*-methyltriazolium (MTA), for the DB24C8 macrocycle shuttling along the thread component through acid-base stimulation [38]. In the initial state, the DB24C8 macrocycle rests on the DBA site, the hydrophilic group is far away from the hydrophobic group and the terminal of the molecular

* Corresponding author.
E-mail address: zqcao@henau.edu.cn (Z. Cao).

https://doi.org/10.1016/j.cclet.2024.110353
1001-8417/

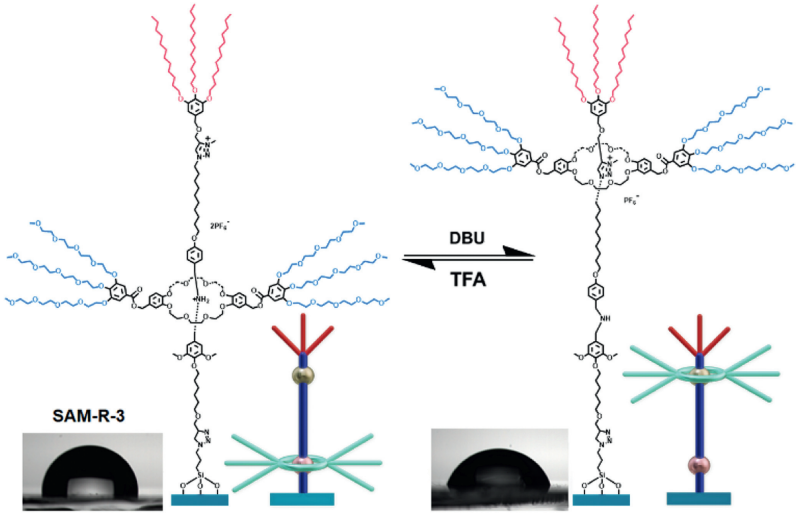

Scheme 1. Cartoon representation of amphiphilic [2]rotaxane shuttle on surface driven by acid-base.

shuttle is hydrophobic, therefore the surface has a higher contact angle. Then the DBA site is deprotonated by the addition of 1,8-diazabicyclo[5.4.0]undec–7-ene (DBU), and the DB24C8 macrocycle shuttle towards the MTA site. The hydrophilic chains on the macrocycle surround the terminal hydrophobic alkyl chains, leading to the decrease of surface contact angle. This work realizes the macroscopic performance contact angle changes through microscopic molecular motion. Thus, the AMMs could control the surface wettability respond to external stimuli.

The synthetic route of the target [2]rotaxane **R-3** was shown in Fig. 1. Firstly, the key intermediate **R-1** was synthesized through the classic threading and blocking method among compounds **1**, **2**, and **3**, which involves a copper(I)-catalyzed Huisgen1,3-dipolar cycloaddition reaction. Then the intermediate **R-2** was obtained in 81% yield after the esterification reaction between **R-1** and compound **4** in the presence of DMAP and EDCI, followed by re-protonated with HCl and anion exchanged with saturated NH_4PF_6 solution. Finally, after the methylation of triazole groups and anion exchanging with saturated NH_4PF_6 solution, the target rotaxane **R-3** was gained in 64% yield.

The chemical structure of key intermediate **R-1**, **R-2,** and the target [2]rotaxane **R-3** were characterized by ^{1}H NMR, ^{13}C NMR spectroscopy, and MALDI-TOF mass spectrometry. According to previous reports [40], the ^{1}H NMR spectrum of [2]rotaxane **R-3** (Fig. 2) indicated that the hydrophilic DB24C8 macrocycle is located at the DBA recognition site. The MALDI-TOF mass spectrum of [2]rotaxane **R-3** showed a peak at $m/z = 3422.506$, which corresponds to the specie lost one PF_6^- anion ([**R-3**-PF_6^-]$^+$), matching with the calculated value of 3421.989 for $[C_{176}H_{290}F_6N_4O_{51}P]^+$. As a result, all of the above experimental data demonstrated that the target [2]rotaxane **R-3** was successfully synthesized.

Furthermore, ^{1}H NMR was employed to characterize the shuttling movement of the target [2]rotaxane **R-3**. The DBA site was deprotonated and the DB24C8 macrocycle shifted to the MTA station when 2.5 equiv. of DBU were added to the CD_3COCD_3 solution of the target [2]rotaxane **R-3**, as evidenced by chemical shift changes in the ^{1}H NMR spectra (Fig. 2). Further analysis was shown in Fig. 2, the H_9 and H_{12} methylene protons neighboring the MTA station were upfield shifted with $\Delta\delta$ −0.62 and −0.82 ppm, because of the shielding effect with the DB24C8 macrocycle. The H_{10} and H_{11} protons on the MTA station were downfield shifted with $\Delta\delta$ −0.65 and 0.32 ppm, due to the interaction with the DB24C8 macrocycle. What's more, the H_3 and H_4 close to the DBA station were upfield shifted with $\Delta\delta$ −1.02 and −0.91 ppm, respectively,

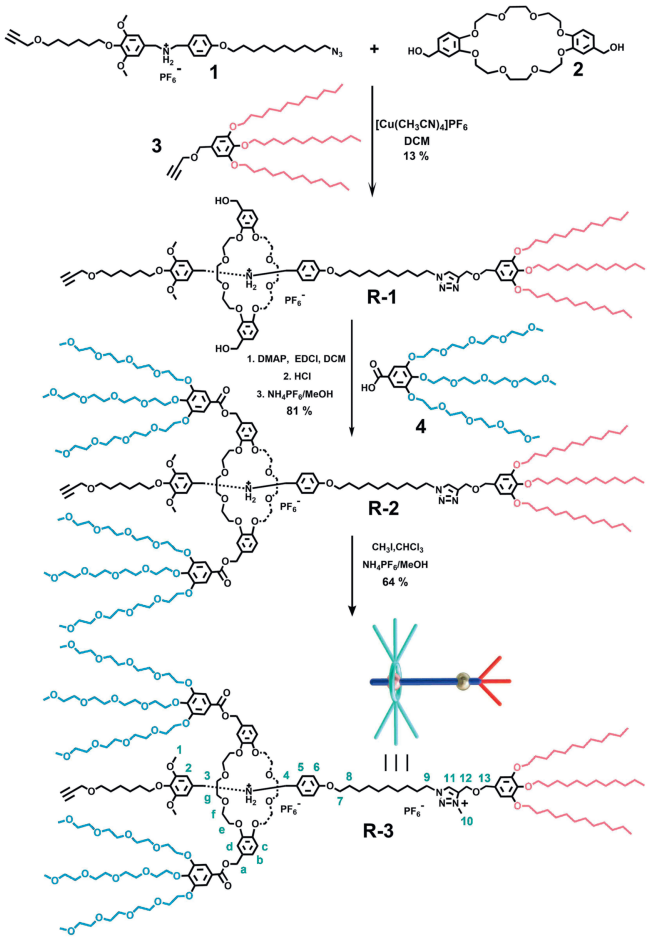

Fig. 1. The synthetic route of target [2]rotaxane **R-3**.

on account of the de-shielding effect with the DB24C8 macrocycle. Next, following the addition of 5.0 equiv. of trifluoroacetic acid (TFA) to the DBU-added solution, the ^{1}H NMR spectra almost recovered to the initial state. This transformation could be explained by the re-protonation of the DBA center and the DB24C8 macrocycle returning to its incipient state. Therefore, ^{1}H NMR spectroscopy confirmed the reversible shuttling motion of the macrocycle along

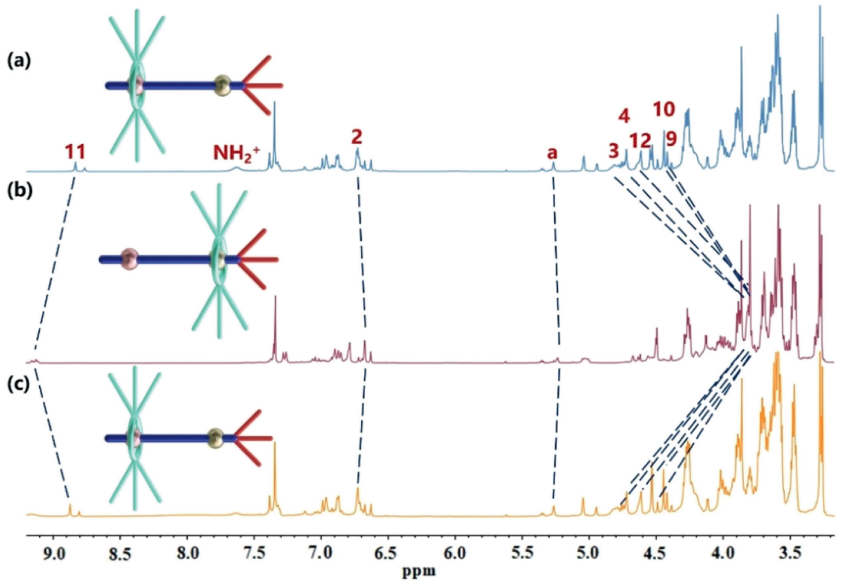

Fig. 2. Partial ^{1}H NMR spectra (400 MHz, CD_3COCD_3, 298 K): (a) [2]rotaxane **R-3** solution, (b) addition of 2.5 equiv. of DBU to the sample a, (c) addition of 5.0 equiv. of TFA to the sample b. The corresponding structures are shown in Fig. 1.

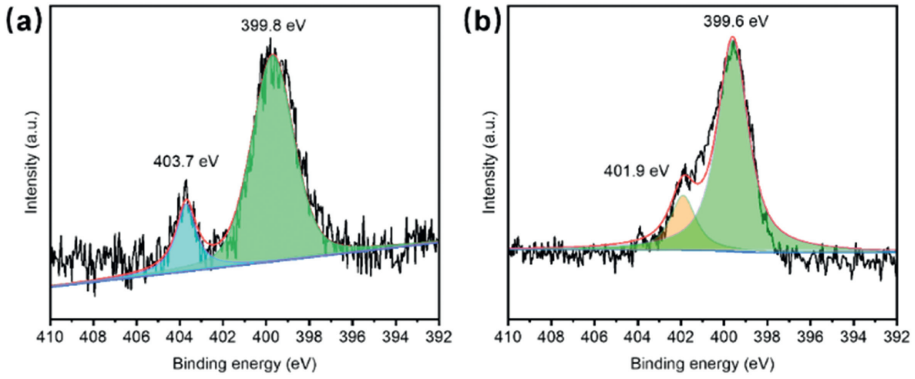

Fig. 3. The XPS N 1s spectrum: (a) azide-functionalized glass surface and (b) **SAM-R-3**.

with the thread component between two distinct sites in [2]rotaxane **R-3** in response to external acid/base stimuli.

At last, in order to achieve the functionalization and materialization of AMMs, the amphiphilic target [2]rotaxane **R-3** was modified onto the glass surface to prepare **SAM-R-3** through classical copper(I)-catalyzed reaction between the azide-functionalized glass surface and the alkynyl-terminal [2]rotaxane **R-3**. To confirm the effective synthesis of the chemical-modified **SAM-R-3**, X-ray photoelectron spectroscopy (XPS) was employed to provide conclusive evidence (Fig. 3). After the click reaction, the XPS N1s spectrum of **SAM-R-3** presented the disappearance of the peak at 403.7 eV to the level of the noise, which indicated the effective click reaction on the azide-functionalized glass surface [26]. Moreover, a new peak at 401.9 eV emerged after the click reaction, which represented the N atoms of the NH_2^+ group in [2]rotaxane **R-3** and certificated the existence of the target [2]rotaxane **R-3** on the glass surface.

Subsequently, the wettability properties of **SAM-R-3** in response to external stimuli were investigated by contact angle. As shown in Fig. 4a, due to numerous hydroxyl groups exposed on the glass surface after being treated with piranha solution, the glass surface displayed obvious hydrophilicity, with a contact angle of 28° ± 1°. The contact angle increased to 75° ± 1° after azide-functionalized silane modification (Fig. 4b), further indicating that the azide-functionalized glass surface has been successfully prepared. After

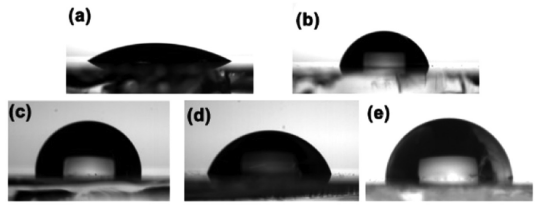

(f)

different stimuli conditions	contact angle (deg)
SAM-R-3	91±1
SAM-R-3 + DBU	69±1
SAM-R-3 + DBU + TFA	90±1

Fig. 4. The change of the contact angle of Glass surface: (a) Glass surface treated by piranha solution, (b) glass surface modified with azide-functionalized silane, (c) **SAM-R-3**, (d) c soaked in DBU solution (CH_2Cl_2, 1.0×10^{-3} mol/L), (e) d soaked in TFA solution (CH_2Cl_2, 1.0×10^{-3} mol/L). (f) The summary table of contact angle changes of **SAM-R-3** under different stimuli conditions.

the click reaction between the azide-functionalized glass surface with [2]rotaxane **R-3**, the contact angle further rose to 91° ± 1° (Fig. 4c) and the surface became a hydrophobic state. This phenomenon demonstrated that the bulky target [2]rotaxane **R-3** was successfully attached to the glass surface, and the terminal hy-

drophobic group can improve the hydrophobic performance. Then the contact angle of **SAM-R-3** decreased to 69° ± 1° (Fig. 4d) after the **SAM-R-3** was immersed in DBU solution (1.0×10^{-3} mol/L) and sonicated for 15 min. The results could be explained by the hydrophilic macrocycle moved to the MTA station under the DBU environment, surrounding the hydrophobic alkyl chain and improving the hydrophilicity of **SAM-R-3**. Finally, DBU-treated **SAM-R-3** was soaked into TFA solution (1.0×10^{-3} mol/L) and sonicated for 15 min, the contact angle almost returned to the initial state 90° ± 1° (Fig. 4e). The contact angle changes of **SAM-R-3** under different stimuli conditions were summaried in Fig. 4f. This results demonstrated that amphiphilic [2]rotaxane modified onto surface could be used to controlling wettability through changing molecular state under an external stimulus.

In summary, we have designed and synthesized an alkyne-terminated amphiphilic [2]rotaxane **R-3** and successfully attached it to the glass surface, as proved by N1s XPS spectrum and contact angle. What's more, the controllable wettability is demonstrated by the contact angle change under acid-base stimuli. The microscopic motion of the AMMs achieves integration and amplification through macroscopic wettability, which lays the groundwork for artificial molecular machine application research. This work is a small step for the development of AMMs towards solid surfaces. It may be used for future artificial intelligent materials.

Declaration of competing interest

The authors declare that they have no known competing financial interests or personal relationships that could have appeared to influence the work reported in this paper.

CRediT authorship contribution statement

Dongpu Wu: Writing – original draft, Investigation, Formal analysis, Data curation. **Zheng Yang:** Investigation. **Yuchen Xia:** Investigation, Conceptualization. **Lulu Wu:** Project administration, Funding acquisition. **Yingxia Zhou:** Supervision, Resources. **Caoyuan Niu:** Project administration, Methodology. **Puhui Xie:** Supervision. **Xin Zheng:** Resources, Methodology. **Zhanqi Cao:** Writing – review & editing, Supervision, Methodology, Investigation, Funding acquisition, Formal analysis, Conceptualization.

Acknowledgments

This work was supported by the National Natural Science Foundation of China (Nos. 21901063, U20041101), Young Talents Personnel Fund of Henan Agricultural University (No. 30500604), Key Science and Technology Foundation of Henan Province (Nos. 242102230178, 232102310379). We acknowledge Molecular Scale Lab for mass spectrometry characterization.

Supplementary materials

Supplementary material associated with this article can be found, in the online version, at doi:10.1016/j.cclet.2024.110353.

References

[1] H. Yang, B. Yuan, X. Zhang, O.A. Scherman, Acc. Chem. Res. 47 (2014) 2106–2115.
[2] Y.Y. Liu, X.Y. Yu, Y.C. Pan, et al., Sci. China Chem. 67 (2024) 1397–1441.
[3] L. Chen, X. Sheng, G. Li, F. Huang, Chem. Soc. Rev. 51 (2022) 7046–7065.
[4] S.Erbas Cakmak, D.A. Leigh, C.T. McTernan, A.L. Nussbaumer, Chem. Rev. 115 (2015) 10081–10206.
[5] L. Feng, R.D. Astumian, J.F. Stoddart, Nat. Rev. Chem. 6 (2022) 705–725.
[6] Y. Li, X. Lou, C. Wang, et al., Chin. Chem. Lett. 34 (2023) 107877.
[7] D. Dattler, G. Fuks, J. Heiser, et al., Chem. Rev. 120 (2020) 310–433.
[8] S. Amano, S.D.P. Fielden, D.A. Leigh, Nature 594 (2021) 529–534.
[9] D.H. Qu, Q.C. Wang, Q.W. Zhang, X. Ma, H. Tian, Chem. Rev. 115 (2015) 7543–7588.
[10] K.Y. Chen, O. Ivashenko, G.T. Carroll, et al., J. Am. Chem. Soc. 136 (2014) 3219–3224.
[11] L. Liu, Y. Liu, P. Liu, et al., Chem. Sci. 4 (2013) 1701–1706.
[12] C. Wang, S. Wang, H. Yang, et al., Angew. Chem. Int. Ed. 60 (2021) 14836–14840.
[13] W.Z. Wang, L.B. Huang, S.P. Zheng, et al., J. Am. Chem. Soc. 143 (2021) 15653–15660.
[14] Q. Zhang, H. Qian, T. Xiao, R.B.P. Elmes, L. Wang, Chin. Chem. Lett. 34 (2023) 108365.
[15] Z. Cao, D. Wu, M. Li, et al., Chin. Chem. Lett. 33 (2022) 1533–1536.
[16] Z. Cao, F. Yang, D. Wu, et al., Polym. Chem. 14 (2023) 1318–1322.
[17] D. Ren, L. Tang, Z. Wu, et al., Chin. Chem. Lett. 34 (2023) 108617.
[18] H. Qian, T. Xiao, R.B.P. Elmes, L. Wang, Chin. Chem. Lett. 34 (2023) 108185.
[19] X.Y. Lou, Y.W. Yang, Adv. Mater. 32 (2020) 2003263.
[20] Z. Li, N. Song, Y.W. Yang, Matter 1 (2019) 345–368.
[21] W. Liu, L.O. Jones, H. Wu, et al., J. Am. Chem. Soc. 143 (2021) 1984–1992.
[22] H. Wu, Y. Wang, C. Tang, et al., Nat. Commun. 14 (2023) 1284.
[23] F.F. Shen, Y. Chen, X. Xu, et al., Small 17 (2021) 2101185.
[24] N. Song, Z. Zhang, P. Liu, et al., Adv. Funct. Mater. 31 (2021) 2009924.
[25] K. Ariga, Chem. Sci. 11 (2020) 10594–10604.
[26] Z.Q. Cao, Q. Miao, Q. Zhang, et al., Chem. Commun. 51 (2015) 4973–4976.
[27] L. Feng, Y. Qiu, Q.H. Guo, et al., Science 374 (2021) 1215–1221.
[28] F. Geyer, M. D'Acunzi, A. Sharifi-Aghili, et al., Sci. Adv. 6 (2020) eaaw9727.
[29] X. Chen, M. Wang, Y. Xin, Y. Huang, Surf. Interfaces 31 (2022) 102022.
[30] V. Parkula, M. Berto, C. Diacci, et al., Anal. Chem. 92 (2020) 9330–9337.
[31] M. Wang, H. Li, Q. Xin, et al., Appl. Surf. Sci. 638 (2023) 158075.
[32] M. Ugrinic, A. deMello, T.Y.D. Tang, Chem 5 (2019) 1727–1742.
[33] N.Y.J. Tan, X. Zhang, D.W.K. Neo, et al., J. Manuf. Process 71 (2021) 113–133.
[34] Q. Zhang, D.H. Qu, ChemPhysChem 17 (2016) 1759–1768.
[35] B. Shi, X. Li, Y. Chai, et al., Angew. Chem. Int. Ed. 62 (2023) e202305767.
[36] C. Yang, H. Chen, ACS Appl. Nano Mater. 5 (2022) 13874–13886.
[37] C. Yu, X. Wang, C.X. Zhao, et al., Chin. Chem. Lett. 33 (2022) 4904–4907.
[38] Z.Q. Cao, Y.C. Wang, A.H. Zou, et al., Chem. Commun. 53 (2017) 8683–8686.
[39] J. Yao, X. Fu, X.L. Zheng, Z.Q. Cao, D.H. Qu, Dyes Pigments 121 (2015) 13–20.
[40] S. Di Noja, M. Garrido, L. Gualandi, G. Ragazzon, Chem. Eur. J. 29 (2023) e202300295.